INL/EXT-17-43427

Light Water Reactor Sustainability Program

Enhancements to Engineering-scale Reactor Pressure Vessel Fracture Capabilities in Grizzly

Benjamin W. Spencer
William M. Hoffman
Wen Jiang

September 2017

DOE Office of Nuclear Energy

INL/EXT-17-43427

Light Water Reactor Sustainability Program

Enhancements to Engineering-scale Reactor Pressure Vessel Fracture Capabilities in Grizzly

Benjamin W. Spencer
William M. Hoffman
Wen Jiang

Idaho National Laboratory

September 2017

Idaho National Laboratory
Idaho Falls, Idaho 83415

http://www.inl.gov/lwrs

Prepared for the
U.S. Department of Energy
Office of Nuclear Energy
Under DOE Idaho Operations Office
Contract DE-AC07-05ID14517

ABSTRACT

The Grizzly code is being developed to model the effect of aging in nuclear power plant systems, components, and structures. A significant part of this effort has been to develop capabilities to model the effects of embrittlement in reactor pressure vessels on their integrity. This includes both modeling of microstructure and engineering property evolution, and engineering-scale probabilistic fracture mechanics analysis. This report documents recent advances to the engineering-scale fracture mechanics capability for evaluation of RPV integrity under transient loading in Grizzly. These developments are in three areas: probabilistic fracture mechanics, general reduced order models for fracture a flaw locations, and improvements to the XFEM capability used in Grizzly for fracture mechanics analysis. The combination of these developments brings Grizzly closer to a state where it can be applied in production as a general tool for engineering-scale fracture mechanics analysis. The probabilistic fracture mechanics capabilities are included in the 1.5 testing version of Grizzly, and will be further refined in preparation for production use in the 2.0 released planned for fiscal year 2018.

CONTENTS

FIGURES

ACRONYMS

CSV	comma-separated value
DOF	degree of freedom
EONY	Eason Odette Nanstad and Yamamoto
LEFM	linear elastic fracture mechanics
LWR	light water reactor
LWRS	Light Water Reactor Sustainability
MPI	Message Passing Interface
PFM	probabilistic fracture mechanics
RISMC	Risk-Informed Safety Margins Characterization
RPV	reactor pressure vessel
SIF	stress intensity factor
SIFIC	stress intensity factor influence coefficient
XFEM	extended finite element method

1 Introduction

The Grizzly code is being developed under the Risk-Informed Safety Margin Characterization (RISMC) Pathway in the U.S. Department of Energy's Light Water Reactor Sustainability (LWRS) program. Grizzly simulates aging mechanisms and predicts the capacity of aged systems, structures, and components in existing light water reactor (LWR) nuclear power plants. The overarching goal of this effort is to make the use of physics-based models accessible, and improve confidence in predictions of the effects of aging. This will permit better-informed decision making as long term operation of plants is considered.

The primary focus of Grizzly development has been on aging mechanisms and capacity of reactor pressure vessels (RPVs). The primary concern in considering the integrity of an RPV during a transient event is that fracture may initiate at the location of a pre-existing flaw introduced during the manufacturing process. Over time, exposure to irradiation and elevated temperature embrittles the material, making it more susceptible to fracture. Efforts are being made both to model the microstructure and engineering properties of RPV steel, as well as to develop a modern, flexible tool for engineering analysis of RPVs subjected to transients.

This report documents recent work on the engineering-scale fracture mechanics modeling capabilities in Grizzly directed at prediction of fracture of RPVs during transient loading scenarios. There are three main development activities documented here:

- *Probabilistic fracture mechanics capabilities* A prototype implementation of a procedure for performing probabilistic fracture mechanics simulation of a RPV containing a population of flaws was documented in [1]. This capability has now been included in the Grizzly code base and included in a recently tagged version 1.5 of the code. Significant improvements have been made to make this capability more flexible, usable, testable, and efficient.

- *Reduced order models for general flaw geometries* Current practice is to consider only flaws that are aligned in the axial or circumferential orientation relative to the RPV. Grizzly is developed as a general tool that can be used to consider local geometric effects and more general flaw geometries. An ability to efficiently evaluate off-axis flaws or other flaw geometries in a probabilistic fracture simulation will greatly expand the applicability of this tool. A procedure to generate reduced order models to efficiently evaluate general flaw geometries has been developed and is demonstrated here.

- *Improvements to XFEM method for mesh-independent fracture simulations* The extended Finite Element Method (XFEM) is used by Grizzly to perform fracture mechanics calculations of arbitrary flaw geometries. The implementation of XFEM has been expanded to include the effects of higher-order terms in the solution fields near the crack tip. This allows for a smoother and more accurate solution with a coarser finite element mesh in the vicinity of the flaw.

These developments are being made to prepare Grizzly for use as a flexible, general tool for engineering fracture mechanics analysis of RPVs.

2 Probabilistic fracture mechanics

An important part of a comprehensive capability for assessing the integrity of RPVs under transient loading is an ability to perform probabilistic fracture mechanics (PFM) analysis to determine the probability of failure of an RPV containing a population of flaws. An initial demonstration of a capability was demonstrated in [1]. This was a proof of concept, and was not yet included in the Grizzly code base.

The PFM capability is comprised of three major components: a capability to evaluate the global thermomechanical response of an RPV under transient loading conditions, a random sampling tool to generate realizations of flaw populations with appropriate distributions of geometric, chemistry, fluence, and other material characteristics, and finally, an ability to efficiently evaluate the probability of failure of a specific flaw subjected to far-field stresses (computed by the global RPV response model).

Significant changes have been made to the procedures used for random sampling of the flaw population and for evaluating the failure probability of individual flaws. The original implementation described in [1] was based on a custom sampler class developed based on the RAVEN code, and used a Python module to evaluate the probability of failure of individual flaws. The new version included in Grizzly is now based entirely on code built into Grizzly. This new version has the following advantages over the previous implementation:

- *Flexibility*: The Python plugin originally developed to evaluate failure probabilities only permitted the use of a specific set of techniques to obtain the far-field stresses from a global RPV model and evaluate failure probabilities. Because of the architecture of the code, it was difficult to transfer parameters to control the way models were evaluated. The new system is based on a modular architecture, which will be described here, and which allows great flexibility in how a number of aspects of the model are evaluated.

- *Integration with other Grizzly capabilities*: The new system is completely built into the Grizzly code base, and is tested and maintained together with the rest of Grizzly, rather than being spread across two very different code bases, which made code maintenance and testing difficult. It allows for natural incorporation of models used in Grizzly into the PFM evaluation procedure. The new system also uses only the MOOSE input syntax, rather than a combination of the very different input syntax of the MOOSE and RAVEN codes.

- *Computational efficiency*: The PFM evaluation procedure involves the evaluation of a very large number of individual flaw failure probability calculation models. Each one of these models typically requires little run time (a fraction of a second), so the process of setting up and launching the individual jobs incurred a significant overhead. The path to parallel scalability on distributed memory computers for this problem with an architecture tailored toward launching more heavyweight models was not clear. The new implementation is based on an architecture that does not have those overheads, and can achieve optimal parallel scalability through its use of the Message Passing Interface (MPI).

The details of the components of the PFM capability in the Grizzly 1.5 release are described in this section.

2.1 Global RPV Thermomechanical Response Modeling

Previous work has demonstrated Grizzly's ability to compute the coupled thermal and mechanical response of a RPV subjected to a transient loading event. One of Grizzly's strengths is that it can model geometries of arbitrary dimensionality, which allows it to capture local variations in the response that can only be captured with higher-dimensional models. For the common case in which only the beltline region of the vessel is

evaluated under uniform temperature conditions, a 1D model is adequate. Previously, Grizzly only had the capability for 2D or 3D global RPV models, and a single strip of 2D axisymmetric elements with appropriate boundary conditions was used to model the beltline region as an infinite cylinder. In the last year, a capability was added for 1D axisymmetric models with an appropriate constraint to correctly model the axial response.

2.2 Random Sampling and Model Execution

The random sampling procedure used by Grizzly for PFM analyses is based on recently-developed capabilities in the MOOSE framework. MOOSE has had the ability for a model to run sub-models for various purposes for some time using a system known as MultiApps. This system allows for a master model to create and run arbitrary numbers of sub-model for a variety of purposes, using the same set of MPI processes used in the master analysis. This system allows for a variety of types of data to be transferred to and from the sub-models, including field, vector, and scalar data.

Recently, a system for sampling of random variables was added to MOOSE. A Sampler class generates a set of randomly sampled variables, and interfaces with an arbitrary number of Distribution objects to transform randomly generated variables to conform with desired distributions. Once the set of samples is generated, a Transfer and MultiApp object specialized for use with random sampling create sub-models for each of the random samples, transfer inputs to those models, execute them, and transfer results back to the master application. The master application does not necessarily need to solve a finite element model, and can simply serve as a controller for randomly sampling variables.

For sampling of variables pertinent to RPV PFM analysis, a specialized class called RPVFractureSampler was developed in Grizzly that follows the sampling protocol used by the FAVOR code, described in [2] and [1]. A set of random variables describing the dimensions, location, type, and orientation of each flaw is generated. In addition, variables defining the chemistry of the RPV steel in the vicinity of the flaw are generated, defined using the concentrations of Cu, Ni, Mn, and P. The neutron fluence is also generated, as well as the initial ductile to brittle transition temperature. Although a Monte Carlo sampling scheme is used, the procedures for sample generation are specialized for this application, and this cannot be done with a generic Monte Carlo sampler.

The number of flaws and the distributions of size and depth of the flaws are defined in tabular data read from files. Chemistry distributions are sampled once per plate or weld subregion of the vessel, and additional distributions are used for local variations in those characteristics.

2.3 Failure Probability Evaluation of Individual Flaws

Computing the probability of failure of an individual flaw involves a number of steps. The time history of the stress intensity factor at the flaw tip must be computed. Because the temperature has a strong effect on the fracture toughness, it must also be computed at that location. The embrittlement, measured as a shift in the ductile to brittle transition temperature, is also computed at that location. Once that information is all available, the probability of fracture initiation at any given time can be computed using a Weibull model and the fracture master curve.

There are multiple ways each of the components of this calculation can be performed. For instance, a variety of reduced order models are employed for evaluating the stress intensity factor for various flaw geometries based on the far-field stresses, which themselves can be obtained in several different ways from the global model. This could also potentially be evaluated using a detailed computational fracture mechanics model in some cases. Embrittlement could be calculated using a number of different models. Neutron fluence could be computed using a simple attenuation model, or potentially using a detailed neutron transport model of a RPV.

To allow for code users to flexibly define the set of models used in these calculations, a modular set of objects was developed for the probabilistic fracture calculation in Grizzly. Figure 1 shows a diagram of these major types of objects, with their dependencies.

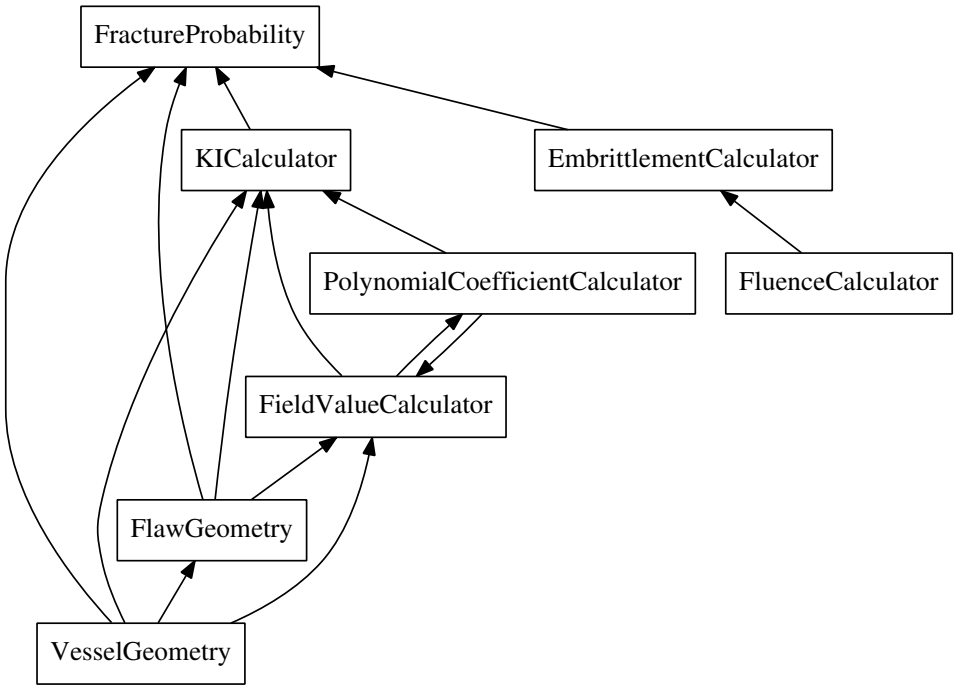

Figure 1: Dependency graph of objects used in fracture probability calculation

The MOOSE framework that Grizzly builds on is written in C++, and uses a modular design where developers add capabilities by implementing specific classes based on base classes. The design for this probabilistic fracture mechanics capability follows that pattern, and defines a set of base classes from which specialized classes are derived. Figure 2 shows a diagram of the set of base classes used to define the interfaces to the various components of this capability along with the derived classes that provide implementations of specializations of these capabilities. Summaries of these classes are described below.

2.3.1 VesselGeometry

The VesselGeometry object is required in a PFM analysis, and is used as a means for the user to define basic characteristics of the RPV geometry, such as its radius, wall thickness, and cladding thickness. This is used by multiple other objects, which call functions on this object to obtain those properties.

2.3.2 FlawGeometry

The FlawGeometry object is also required in a PFM analysis, and is used to define geometric characteristics of the specific flaw being considered, such as flaw depth, aspect ratio, and orientation. Like VesselGeometry, this is used by other objects, which call functions on this class to get those properties.

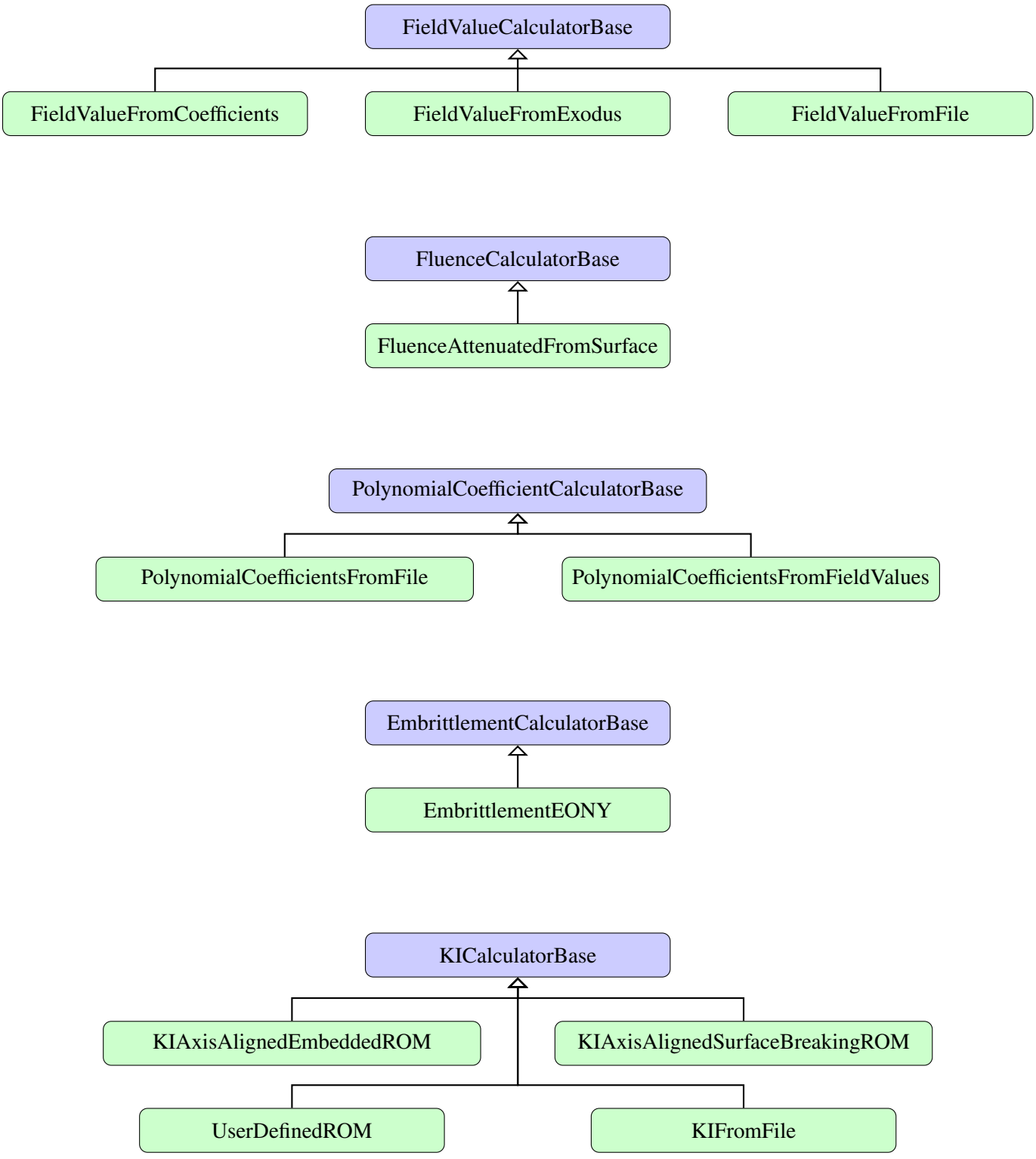

Figure 2: Inheritance diagram for specializations of classes used in fracture probability calculation

2.3.3 FieldValueCalculator

The FieldValueCalculator calculates the value of a solution field variable in the global thermo-mechanical model at a specific location. There are several ways this can be obtained, so a base class is created to define a common interface to these objects. This is used by multiple other objects to obtain local stresses and temperatures.

FieldValueCalculatorBase This is the base class that defines the interface to all FieldValueCalculator objects. Other objects that depend on this object call a function on this class to obtain the value of the field at a specified depth.

FieldValueFromCoefficients This class uses coefficients of polynomial fits to a given field as a function of the depth. These coefficients are obtained from a class derived from PolynomialCoefficientCalculatorBase.

FieldValueFromExodus This class computes the value of an arbitrary field that is read from a binary Exodus file (the standard format for the output file written by Grizzly or other MOOSE-based applications). The solution field is interpolated to the point where it is requested. This can be used to read results from an arbitrary 1D, 2D, or 3D global solution.

FieldValueFromFile This class obtains the value of a solution field from a comma separated value (CSV) formatted text file, which contains values that only vary in time. Because the solution cannot vary spatially, this is primarily useful for evaluations of a single flaw where the depth is known in advance. The global Grizzly analysis can output a CSV file containing the history of a field value at a specific location using a Postprocessor.

2.3.4 PolynomialCoefficientCalculator

The PolynomialCoefficientCalculator computes the coefficients for a polynomial of arbitrary order defining the variation of a field through the thickness of the vessel as a function of depth.

PolynomialCoefficientCalculatorBase This is the base class that defines the interface to all Polynomial-CoefficientCalculator objects. Other objects that depend on this object call a function on this class to obtain the coefficients.

PolynomialCoefficientsFromFile This class provides access to polynomial coefficients that are stored in a CSV-formatted text file. This file contains a set of columns of data, where each column contains the polynomial coefficients for a given time step. These files can be generated by using VectorPostprocesors that perform least-squares fits of polynomials to sampled field variables in the global RPV model.

PolynomialCoefficientsFromField This class uses a FieldValueCalculator object to sample the value of a field at various depths, and perform a least-squares fit on that data to compute coefficients for a polynomial for a given time. This allows the use of reduced order models for stress intensity factor calculations that rely on polynomial coefficients in cases where the global solution is obtained from an Exodus file.

2.3.5 FluenceCalculator

The FluenceCalculator computes the neutron fluence at a given depth.

FluenceCalculatorBase This is a base class that provides the interface to all classes (currently just one) that provide the fluence at a given depth.

FluenceAttenuatedFromSurface This class uses an exponential attenuation law to compute fluence at a specified depth by multiplying the attenuation factor by the fluence at the surface.

2.3.6 EmbrittlementCalculator

The EmbrittlementCalculator computes the embrittlement as a shift in the ductile to brittle transition temperature.

EmbrittlementCalculatorBase This is a base class that provides the interface to all classes (currently just one) that compute the embrittlement as a function of a number of factors, including chemistry, temperature, and fluence.

EmbrittlementEONY This class uses the EONY model [3] to compute the embrittlement. This is a physically-based, empirically correlated model.

2.3.7 KICalculator

The KICalculator computes the mode-I stress intensity factor, K_I, as a function of applied far-field stress in the global model.

KICalculatorBase This is the base class that defines the interface to all KICalculator objects.

KIAxisAlignedEmbeddedROM This class uses closed-form solutions to compute K_I for embedded flaws.

KIAxisAlignedSurfaceBreakingROM This class uses closed-form solutions to compute K_I for surface-breaking flaws.

UserDefinedROM This class uses user-defined stress coefficients for the dependence on axial, hoop, and radial stress defined in a CSV-formatted text file to compute K_I by multiplying those coefficients by the coefficients to polynomial fits of those stresses.

KIFromFile This class directly reads the solution for K_I from a CSV-formatted text file. This is useful for testing other components of the model, or for cases where a solution might be obtained from an external code.

2.4 Benchmarking Fracture Solutions

Following the preliminary work presented in [1], a significant effort was undertaken in conjunction with the FAVOR development team to benchmark the Grizzly fracture mechanics solutions against FAVOR solutions. A large number of scenarios for flaw geometry was considered, and as a result of this work, a number of corrections were made to the Grizzly implementation. With the exception of a few scenarios, where the reasons for the discrepancies are well understood, these results match very closely with the FAVOR solutions. A subset of these results is shown in Appendix A.

3 General reduced order model for fracture solutions

Due to the probabilistic nature of these types of problems, a fast and effective means for evaluating flaw stress intensity factors in the reactor pressure vessel wall is essential. Full scale transient RPV simulations with only one flaw can take several hours of computing time, so a vessel realization with potentially thousands of flaws is, for all intents and purposes, too big to evaluate in a way that is useful. Model order reduction can therefore be extremely useful in the context of this problem. Specifically, probabilistic analyses would require a very fast model that could be used to evaluate the stress intensity factor of any particular flaw, for any transient event, in the thick, curved wall of the RPV.

Currently, the Fracture Analysis of Vessels – Oak Ridge (FAVOR) code is used to do similar analyses. FAVOR can be used to conduct Monte Carlo simulations of flawed RPVs in order to determine the probability of vessel failure. The FAVOR code has some limitations, however. One, in particular, is that it is limited to the analysis of flaws that are aligned with the axes of the RPV (axial/circumferential). While it is likely that these flaws are large contributors to the overall probability of failure of the vessel, laminar and off axis flaws could also have a significant effect on structural integrity of the vessel. Therefore, developments within the Grizzly code have been made in order to accommodate flaws of any orientation within the vessel wall.

The FAVOR code utilizes a reduced order model (ROM) in order to perform millions of successive flaw evaluations necessary for Monte Carlo simulations. The code has undergone years of benchmarking efforts and is widely seen and used as a fully verified and validated code. It is therefore a useful benchmarking tool in the early developments of Grizzly's RPV PFM capabilities. Specifically for benchmarking the implementation of a ROM for axis aligned flaws. After demonstrating that Grizzly can be used to evaluate axis aligned flaws, FAVOR's methodology can be extended to flaws of any orientation and implemented within Grizzly.

3.1 Axis Aligned Reduced Order Model

The reduced order model used in the FAVOR code for determining the stress intensity factor for surface breaking, axis-aligned flaws is a deterministic approach utilizing the principle of superposition. It was initially shown [4], under the assumption of Linear Elastic Fracture Mechanics, that this principle could be applied to fracture models such that when combined with a weight function, it created a reduced order model approximating a flaw's stress intensity factor. The resulting model requires two essential components: function weights, and stress intensity factor influence coefficients (SIFICs). The reduced order model equation used for stress intensity factor approximations within FAVOR is shown below, where K_I is the mode-I stress intensity factor, w_i are the function weights, K_i are the SIFICs and a is the depth of the flaw.

$$K_I = \sum_i^n w_i K_i \sqrt{\pi a} \tag{1}$$

At the simplest level, the stress intensity factor is determined as a function to two components, flaw geometry and loading. It should come as no surprise then that, as illustrated by the equation above, this ROM essentially requires two key components. The SIFICs (K_i), which represent geometric effect on the solution, and the function weights (w_i), which capture the specific loading of interest. The ROM is simply the method used to combine the effects of flaw and RPV geometry with the transient loading conditions of interest.

Obtaining function weights requires the development of the global RPV finite element model. This is a model of the uncracked RPV wall, which is used to measure the RPV's response to any thermomechanical boundary conditions of interest. Using this model, the stresses normal to the hypothetical flaw in the RPV wall are obtained at various radial positions throughout the entire wall thickness. The function weights are then obtained by creating a polynomial describing the stress as a function of radial position in the wall,

where the coefficients are then used as the function weights. For FAVOR, a third order cubic polynomial was determined to sufficiently capture the stress distribution in the RPV wall [2] and was therefore implemented into the Grizzly code as well.

The required SIFICs are generated in large quantities beforehand, and are parameterized in a database such that the library of values is representative of a wide array of geometry characteristics. These characteristics include relative flaw depth, flaw aspect ratio, RPV dimensions - any geometric property of the RPV flaw model that would affect the stress intensity solution. Therefore, in order to evaluate the ROM shown in Equation 1, SIFICs must be generated for the crack and RPV geometry of interest.

The process for generating SIFICs comes at an initial cost in terms of computation and depends on the desired scope of flaw geometry. However once created, the values are stored in a database for repeated and rapid use. SIFICs are obtained by creating finite element models of a cracked portion of the RPV wall, hereafter referred to as sub-models. In each sub-model, the geometry of the flaw and RPV are pre-determined and physically represented. Recall that the crack opening stresses are captured using the coefficients from a cubic polynomial. Therefore, for a single axis aligned flaw, four SIFICs are required. Thus, a series of unit pressure loads corresponding to each term in the cubic polynomial is individually applied to the crack face of each sub-model, representative of the loading shown in Figure 3 below. The sub-model is evaluated four different times with the four loads shown below in order to create the four required SIFICs. This process can then be repeated for varying geometric parameters so as to create a library of values that can then be used repeatedly for evaluation in the ROM.

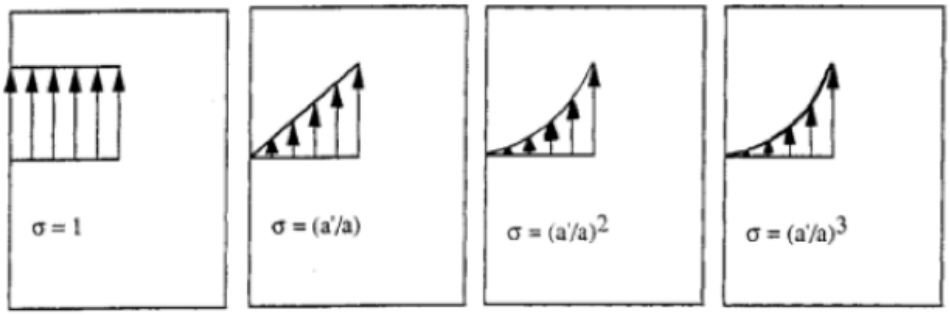

Figure 3: Four separate pressure loads applied for SIFIC generation

Once a library of SIFICs has been created, the global RPV model is evaluated and the coefficients describing the through wall RPV stress are obtained. These coefficients are constant in Equation 1 for any flaw so long as the loading of interest does not change. For Monte Carlo analysis, sampled geometric flaw and RPV characteristics are used to determine the appropriate SIFICs for use in the ROM. If the specific geometric condition is not captured in the SIFIC database, various schemes such as interpolation may be used for approximations.

3.2 Off Axis Reduced Order Model

The approach described above is the method used currently in the FAVOR code for axis aligned flaws. This capability has already been implemented in Grizzly and benchmarked against the FAVOR code (see appendix). As it was mentioned previously, the probabilistic fracture mechanics implementation in Grizzly will include the capability to analyze flaws of any arbitrary orientation. To do this, a ROM capable of accommodating flaws of any orientation is required, and can be developed using the same principle utilized in the axis aligned ROM.

For flaws aligned with the central axes of the RPV, cracks experience mode 1 loading, where either the axial or circumferential stress is the only stress inducing crack opening. Such is not the case for a tilted flaw. Arbitrarily defined flaws that do not align with the RPV axes are subject to opening stresses from all three components of stress in the RPV wall. A reduced order model aiming to measure the stress intensity factor for such a flaw must therefore capture the effects of the loading in all three directions (axial, circumferential, and radial). This means, for a single off axis flaw, 12 SIFICs will be required, as opposed to just four for an axis aligned flaw.

For an axis aligned SIFIC sub-model, the loading is executed as shown in Figure 3 above. A Circumferential flaw will require four pressure loads applied in the axial direction. Because the flaw is perfectly normal to the axial stress, it is the only stress that affects the stress intensity solution, even though there are other stresses induced in the model. For an off axis flaw, stresses in all three directions have an effect on the solution. Therefore, SIFICs cannot be determined by simply applying a simple pressure load to the outer surface of the model as they were for axis aligned flaws. Instead, the stress state must be fixed such that the only non-zero stress in the sub-model exists in only one direction. The magnitudes of the stresses being induced are identical to those shown in Figure 3, however they must exist independently and exclusively within the sub-model at each instant and must be applied in the axial, circumferential and radial directions.

The application of this loading is not as straightforward as simply applying surface pressure loads to the crack face in each sub-model. Because the loading must be purely uni-directional for every SIFIC, Poisson's effect will need to be accounted for, or more specifically, counteracted. Instead of applying external loads, the stress state for each of the desired conditions is set by manually assigning the incremental strain to the desired value in every direction. For the case where a purely axial stress state is required the following strains are set:

$$\begin{aligned} \sigma_{zz} &= f(r)/E \\ \sigma_{rr} = \sigma_{\theta\theta} &= \frac{-\nu * f(r)}{E} \\ &\text{where} \\ f(r) &= (r/R)^n \\ \text{for } n &= 0, 1, 2, 3 \end{aligned} \tag{2}$$

The non-zero component can then be changed for each of the three directions in order to obtain all 12 SIFICs.

Unfortunately, the loading procedure described above is only valid for stresses in the Z direction. This is illustrated by equations of equilibrium in cylindrical coordinates, which are shown below:

$$\begin{aligned} \frac{\partial \sigma_{rr}}{\partial r} + \frac{1}{r}\frac{\partial \sigma_{r\theta}}{\partial \theta} + \frac{\partial \sigma_{rz}}{\partial z} + \frac{\sigma_{rr} - \sigma_{\theta\theta}}{r} + f_r = 0, \\ \frac{\partial \sigma_{r\theta}}{\partial r} + \frac{1}{r}\frac{\partial \sigma_{\theta\theta}}{\partial \theta} + \frac{\partial \sigma_{\theta z}}{\partial z} + 2\frac{\sigma_{r\theta}}{r} + f_\theta = 0, \\ \frac{\partial \sigma_{rz}}{\partial r} + \frac{1}{r}\frac{\partial \sigma_{\theta z}}{\partial \theta} + \frac{\partial \sigma_{zz}}{\partial z} + \frac{\sigma_{rz}}{r} + f_z = 0, \end{aligned} \tag{3}$$

Because this is a cylindrical vessel wall, the nonzero stress components are principal stresses aligned in the r, theta, and z directions. Neglecting body forces, the equations reduce to the single non-trivial equation shown below:

$$r\frac{\partial \sigma_{rr}}{\partial r} = \sigma_{\theta\theta} - \sigma_{rr} \tag{4}$$

The equation above shows that in order for the vessel wall to be in a state of equilibrium, radial stress cannot exist without circumferential stress. Note that the axial stress (z direction) is not included in this relation, and is thus the reason Equations 2 are sufficient for axial loading.

In order to counteract this relationship between the radial and hoop stresses, an artificially imposed body force can be applied to cancel out the unwanted stress component. If the body force term is included in Equation 4, the result is:

$$r\frac{\partial \sigma_{rr}}{\partial r} = \sigma_{\theta\theta} - \sigma_{rr} - f_r \tag{5}$$

The circumferential and radial force components can then be solved for, as shown below:

$$\begin{aligned} \sigma_{rr} &= \frac{\sigma_{\theta\theta}}{r} - f_r \\ \sigma_{\theta\theta} &= r\frac{\partial \sigma_{rr}}{\partial r} - \sigma_{rr} - f_r \end{aligned} \tag{6}$$

Using the relationships shown above, a body force can be applied in order to negate the unwanted stress.

The flaw sub-models for an off axis flaw are setup containing the flaw and RPV geometry of interest. Zero displacement boundary conditions are prescribed such that the exterior surface of the model does not move. Material strains are set such that the stress state is purely one directional for each of the required 12 steps. When the loading direction is radial or circumferential, the appropriate body force is applied in order to keep the sub-model in equilibrium.

The form of the ROM is unchanged, however, it must now be evaluated for all three directions for a single flaw. This means, the global RPV model must be evaluated to determine stress polynomial coefficients for axial, hoop and radial stresses. The coefficients for each of the three polynomials are then used in Equation 1 along with the respective SIFICs. The result of the 3 equations can be summed in order to determine the K_I, K_{II}, or K_{III} solution, depending on the SIFICs used.

3.3 Demonstration

The process described above has been automated within the Grizzly code, although a database of SIFICs for off axis flaws has not yet been generated. The purpose of this demonstration is to prove the concept. The next steps for implementation would include the generation of an off axis flaw SIFIC library and the development of an interpolation scheme for the approximation of intermediate values.

The following will show the methodology described above in a demonstration of the ROM on a single flaw. Although the ROM was designed for use on off axis flaws, it can also be used to evaluate axis-aligned flaws. Therefore, the off axis ROM will be used to compute the stress intensity solution for an embedded circumferential flaw, then a circumferential flaw that is tilted 5 degrees from the circumferential plane. The results generated using reduced order models will then be compared to similar flaw models evaluated using domain integral solution techniques.

3.4 Axis-Aligned Reduced Order Model Benchmarking

The reduced order model detailed above was developed for off-axis flaws, though it can be used to analyze axis-aligned flaws as well. This is true because axis-aligned flaws only experience mode 1 loading, where stresses in only one direction have an effect on the solution. This means, when the SIFICs are generated, the only non-zero values will be those corresponding to the load that induces crack opening. As seen in Equation 1, if the SIFIC has a zero value, it will have no effect on the overall solution.

Given the process detailed previously in this report, a necessary step is the generation of the SIFICs. The geometry of the SIFIC sub-model was created with FAVOR analyses in mind. Specifically, FAVOR obtains solutions without interpolation for models where the RPV has a wall thickness that is one tenth of the innermost radius, as well as for flaws that have a crack length that is one tenth of the thickness of the vessel wall. Therefore, the inner radius of the vessel was set to be 2.1971m, the wall thickness was set at 0.21971m and the crack depth was set at 0.021971m. The flaw is circular and located directly in the center of the RPV wall.

The analysis was performed using Grizzly's Extended Finite Element Method (XFEM) implementation. Therefore, the physical geometry of the flaw is not shown in the mesh. The mesh was generated using Sandia National Lab's Cubit software, where the area around the flaw was refined significantly in order to obtain an accurate stress intensity factor solution. All outer surfaces are fixed for zero displacement and the loading was set internally as described in the sections above. A section view of half the meshed model used for the SIFIC generation is shown below:

Once the SIFICs have been obtained, the other required component for ROM evaluation is the stress polynomial coefficients, obtained from the global RPV model. There are a number of ways that this can be achieved using Grizzly. The wall of the RPV can be represented with a 1D axisymmetric, 2D, simplified 3D or full scale 3D RPV model. The purpose for using a full-scale 3D RPV model would be to accommodate spatially varying boundary conditions including cooling plumes. For this analysis the model shown below was subjected to the transient temperature and pressure boundary condition history shown in Figure 6

The value of K_I was computed using three methods: the general ROM proposed here, a direct solution of full transient response including the flaw, and the reduced order model for axis-aligned flaws already implemented in Grizzly using standard closed-form semi-analytic equations. The direct solution of the full transient response employs exactly the same finite element model of a section of the vessel that was used for generation of the SIFICs (shown in Figure 5). A comparison of the results from these models is shown in Figure 8. The general ROM and the direct simulation of the global RPV including the fracture produce nearly identical results, which indicates that this reduced order modeling procedure works correctly. The direct simulation results shown here are only for the first part of the simulation, because there is a very high computational cost in evaluating this model for a large number of time steps, and this model had not finished running at the time of writing. There is a discrepancy between these simulation results and the axis-aligned benchmark solution that is still being investigated. This discrepancy is due to a difference between the semi-analytic solution and the finite element model, and not due to the reduced order modeling procedure.

There is a significant benefit in computational efficiency with this approach, even if it is used only to evaluate the transient response of a single flaw. To generate the SIFICs requires running this model through 12 loading configurations (for the 4 terms of the polynomial describing the 3 components of the stress field). A typical transient simulation may require running a model through hundreds of time steps. Once the SIFICs are generated, the computational cost of evaluating K_I for a transient event given the polynomial coefficients from a global analysis is near zero. If a transient consists of more than 12 time steps, there will be a benefit in computational cost from using this procedure. This makes it feasible to consider performing probabilistic analysis of RPVs containing off-axis flaws.

3.5 Off-axis Reduced Order Model Benchmarking

The same model used for the axis-aligned flaw shown in the previous section was used to demonstrate this general reduced order model procedure for off-axis flaws. The flaw was tilted 5 degrees off of the circumferential orientation. SIFICs were generated for K_I, K_{II}, and K_{III} by evaluating those respective quantities under the 12 variations of the far-field stress. The same procedure used for the axis-aligned flaw was applied here to obtain the history of the stress intensity factor using both the reduced order model and the direct solution. Figure **??** shows a comparison of K_I and K_{II} for the two models, evaluated at the point in the flaw

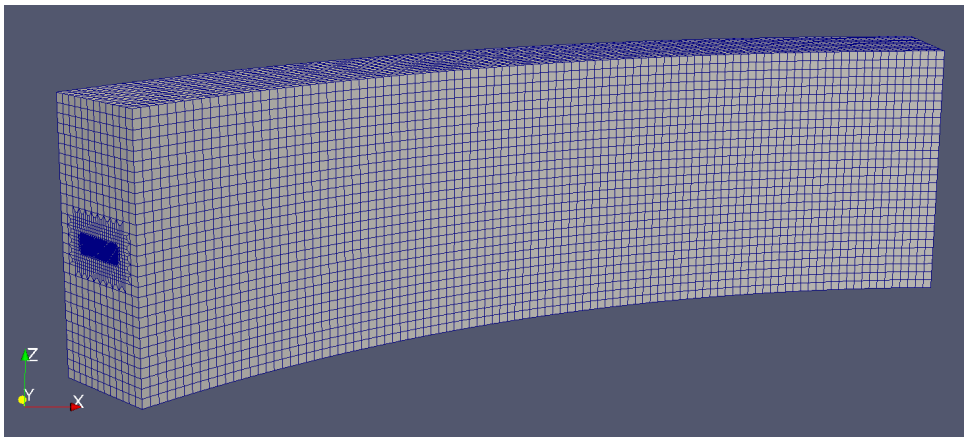

Figure 4: Section view of embedded flaw submodel

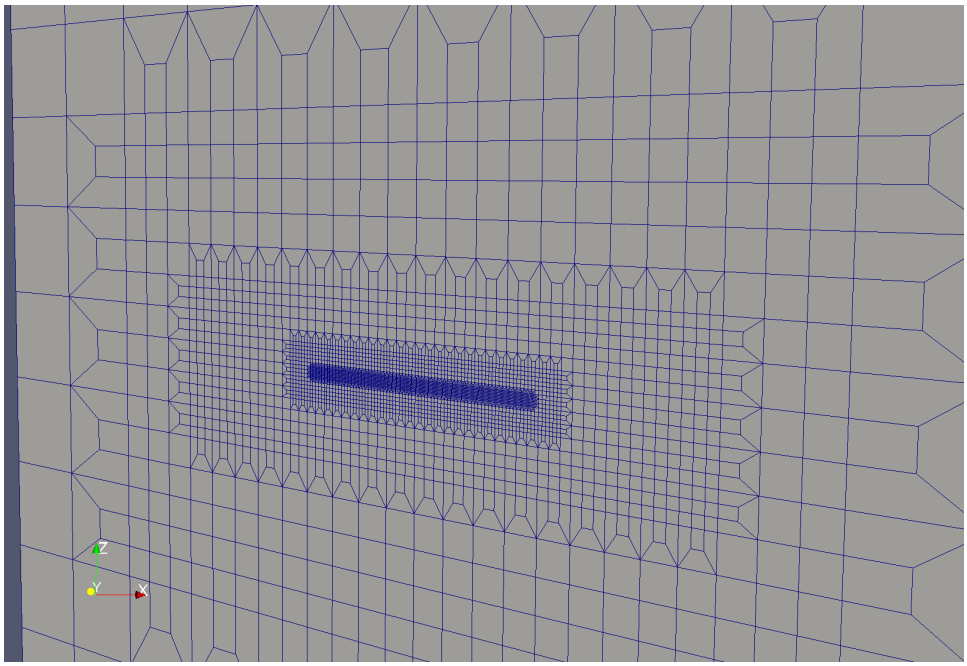

Figure 5: Mesh refinement for flaw model

nearest to the inner surface. K_{III} is not shown here because it is nearly zero. As for the axis-aligned case, the direct simulation was not yet run to completion, but it is evident that the results for both K_I and K_{II} are very close.

These simulations demonstrate that this procedure has the potential to enable very efficient simulation of arbitrary flaw geometries. This procedure still needs to be tested more thoroughly in a wider variety of scenarios. Once confidence is developed in this procedure, procedures can be developed to use response surfaces or similar techniques to generate parameters for this ROM under a variety of conditions.

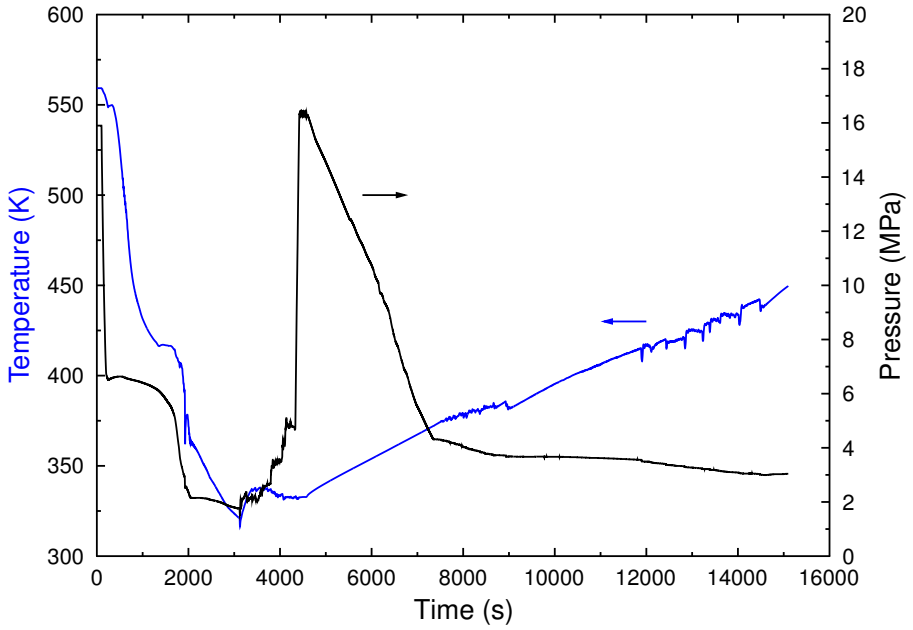

Figure 6: Time history of coolant temperature and pressure applied to RPV

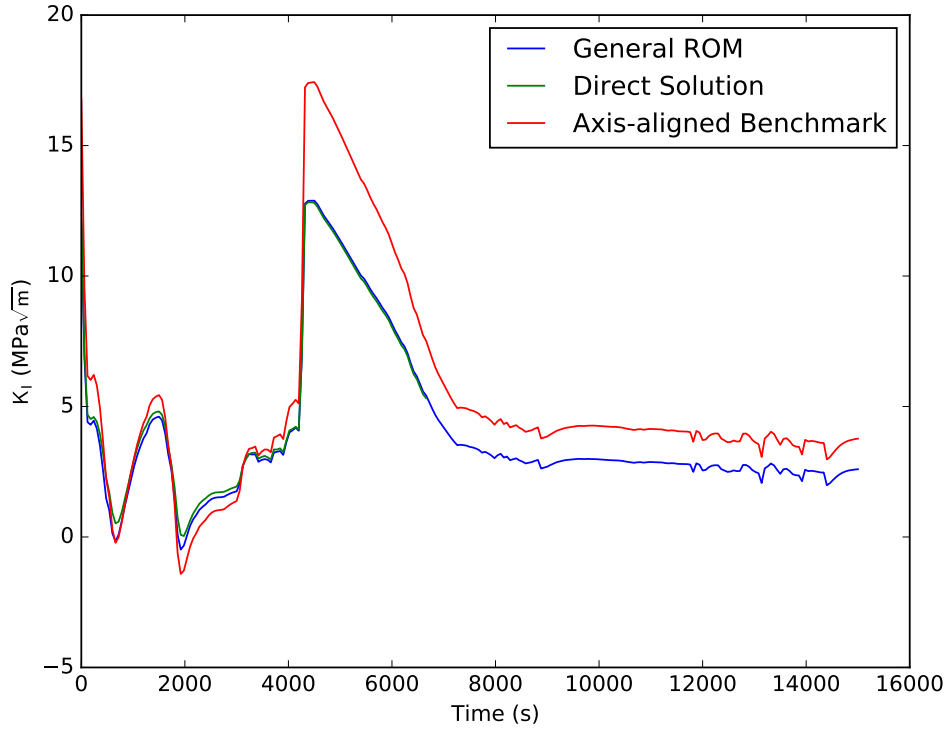

Figure 7: Time history of K_I in axis-aligned embedded flaw computed using three methods: the proposed general reduced order model, a direct simulation, and a benchmark axis-aligned model.

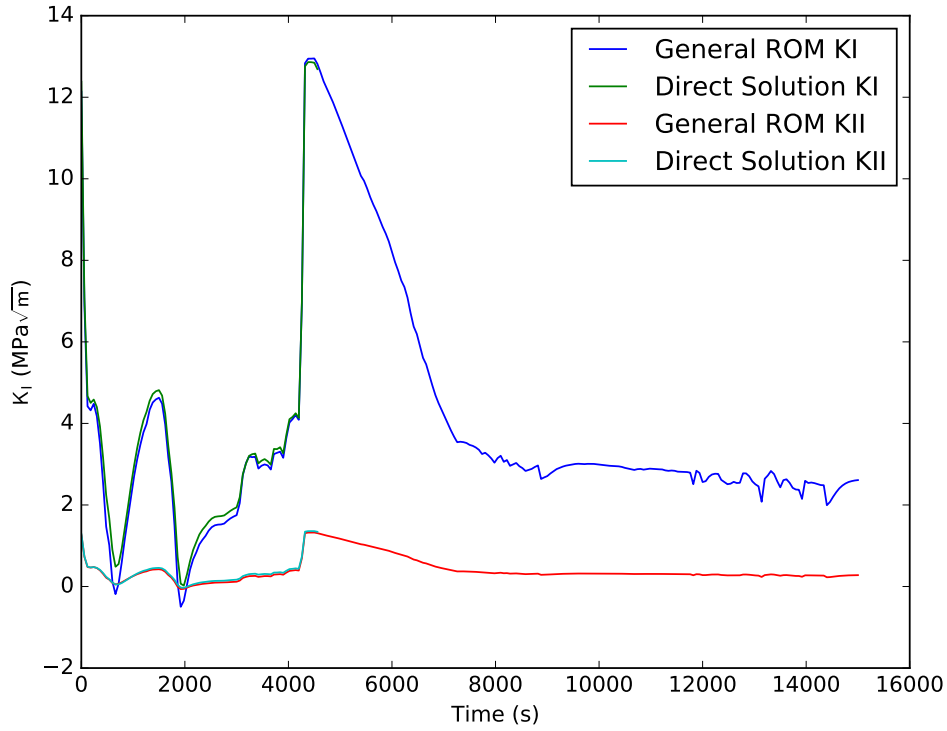

Figure 8: Time history of K_I and $K_I I$ in 5-degree off-axis embedded flaw computed using the proposed general reduced order model, and a direct simulation.

4 Near-tip enrichment in XFEM

4.1 Background

The original X-FEM represents the cracks with enriched shape functions consist of both Heaviside and near-tip asymptotic functions.The initial implementation of the X-FEM in MOOSE is based on the phantom node method which is equivalent to the original X-FEM formulation with Heaviside enrichment. In the phantom node method, the discontinuity is the solution fields is introduced by replacing the cut element with two overlapping "partial" elements that are properly connected to reflect the topology of the crack. With phantom node method, cracks must terminate along element faces. This introduces a somewhat artificial change to the crack front geometry. In addition, the lack of near-tip enrichment reduces the capability of capturing the singular nature of the crack front fields. Thus, for many Grizzly problems, it may be desirable or even necessary to incorporate the near-tip enrichment to improve the accuracy of fracture simulation.

The X-FEM approximation takes the form:

$$\boldsymbol{u}_e^h(\boldsymbol{x}) = \underbrace{\sum_{i\in\mathbb{I}} N_i(\boldsymbol{x})\boldsymbol{u}_i}_{\text{standard FE}} + \underbrace{\sum_{j\in\mathbb{J}\subseteq\mathbb{I}} N_j\boldsymbol{x}H(\boldsymbol{x})\boldsymbol{a}_j}_{\text{discontinuous contribution}} + \underbrace{\sum_{k\in\mathbb{K}\subseteq\mathbb{I}} N_k(\boldsymbol{x})\sum_{\alpha=1}^{4} F_\alpha(\boldsymbol{x})\boldsymbol{b}_{k\alpha}}_{\text{crack-tip contribution}} \tag{7a}$$

with

$$F_\alpha(\boldsymbol{x}) = \sqrt{r}\{\sin\frac{\theta}{2}, \cos\frac{\theta}{2}, \sin\frac{\theta}{2}\sin\theta, \cos\frac{\theta}{2}\sin\theta\} \tag{7b}$$

where $\mathbb{J}$ is the index set of nodes whose basis function support is cut by the interior of the crack and $\mathbb{K}$ is the index sets of nodes whose basis function support contains the crack-tips. In addition, $N_i(\boldsymbol{x})$ are the finite element shape functions, $H(\boldsymbol{x})$ is the generalized Heaviside function (replaced with phantom node method) and $F_\alpha(\boldsymbol{x})$ are the crack-tip asymptotic functions defined with respect to a local crack front polar coordinate system (r, θ) with origin at the crack-tip, see Figure 9. If the crack front is located inside an element, the crack-tip enrichment is required to represent the crack front geometry correctly and improve the accuracy of the stress intensity factor (SIF). It is worth mentioning that $\boldsymbol{u}_i$, $\boldsymbol{a}_j$ and $\boldsymbol{b}_{k\alpha}$ are unknown degrees-of-freedom (DOFs) corresponding to the standard FE, discontinuous and near-tip basis functions, respectively.

4.2 Code development

MOOSE currently does not permit to add variables on a subset of the domain. An in-efficient workaround is to add new variables associated with the enrichment shape functions for the whole mesh and then to simply fix DOFs to zero for those nodes with basis function supports that are far away from any crack tip. This approach is implemented in MOOSE for simplicity and parameter `cut_off_radius` is used to specify the cut-off radius for the enrichment variables. The displacement field $\boldsymbol{u}(\boldsymbol{x})$ now contains both the standard and the enrichment solution. A new `ComputeStrain` Material Class is implemented to calculate the strains from the overall displacements. Additional `StressDivergenceKernel` is also added to obtain the residual and Jacobian contribution from those enrichment variables. The tasks of adding new variables, kernels and boundary conditions are incorporated into `XFEM` Action which greatly facilitates the use of near-tip enrichment.

To accurately evaluate weak form involving those discontinuous functions, additional procedures are needed to perform the numerical integration. Moment-fitting technique has been successfully used on the integration over partial elements in the phantom node method. However, the same technique is not feasible to extend to integrate the discontinuous near-tip enrichment functions. In this work, the accuracy of the integration for those functions is achieved by increasing the order of standard Gaussian quadrature rules.

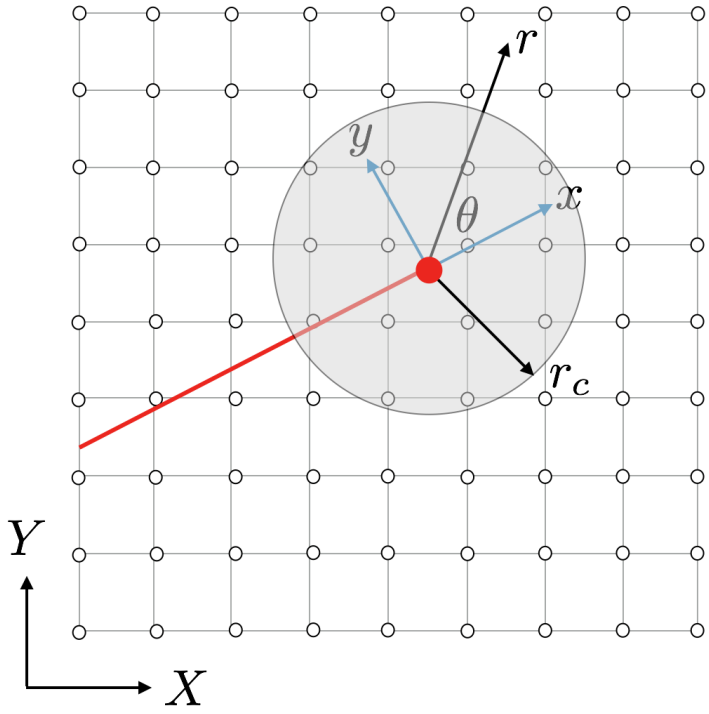

Figure 9: Global and local coordinate system and cut-off radius.

Although it is computationally expensive, it permits the MOOSE to store stateful material properties which are required by most of inelastic materials and large deformation formulation.

4.3 Numerical examples

We look at standard two- and three-dimensional benchmark problems in linear elastic fracture mechanics (LEFM). We use these problems to test our near-tip enrichment implementation and demonstrate that the near-tip enrichment provides better representation of the crack front geometry and result in more accurate results.

4.3.1 2D edge crack

We first consider a 2D plate with an edge crack. This example shown in Figure 10 has dimensions of $W = 1$ and $L = 2$. The pressure σ is prescribed at top and bottom surfaces, respectively. The analytical solution for the SIF is given as:

$$K_I = \sigma\sqrt{\pi a}\left[1.12 - 0.23\left(\frac{a}{W}\right) + 10.6\left(\frac{a}{W}\right)^2 - 21.7\left(\frac{a}{W}\right)^3 + 30.4\left(\frac{a}{W}\right)^4\right] \tag{8}$$

With $a = 0.5$ and $\sigma = 1$, K_I equals to 3.5625. The analytical solution for σ_{yy} is given as a function of K_I:

$$\sigma_{yy} = \frac{K_I}{\sqrt{2.0r\pi}}\cos\left(\frac{\theta}{2}\right)\left[1.0 + \sin\left(\frac{\theta}{2}\right)\sin\left(\frac{3\theta}{2}\right)\right] \tag{9}$$

The convergence study of the L_2 norm of σ_{yy} is shown in the Figure 11a. The convergent rate of the σ_{yy} with near-tip enrichment and without near-tip enrichment is 0.728 and 0.374, respectively. The error is reduced by almost half by adding the near-tip enrichment. It is also shown that the convergent rate of near-tip enrichment becomes smaller as the element size is reducing. This might be attributed to the fact that the error introduced in the integration over the crack tip element brings an ineluctable effect on the overall accuracy. In addition, the convergence study of the J-Integral is shown in Figure 11. It is shown that the J-integral with near-tip enrichment is much better than the one without enrichment, particularly on a coarse mesh.

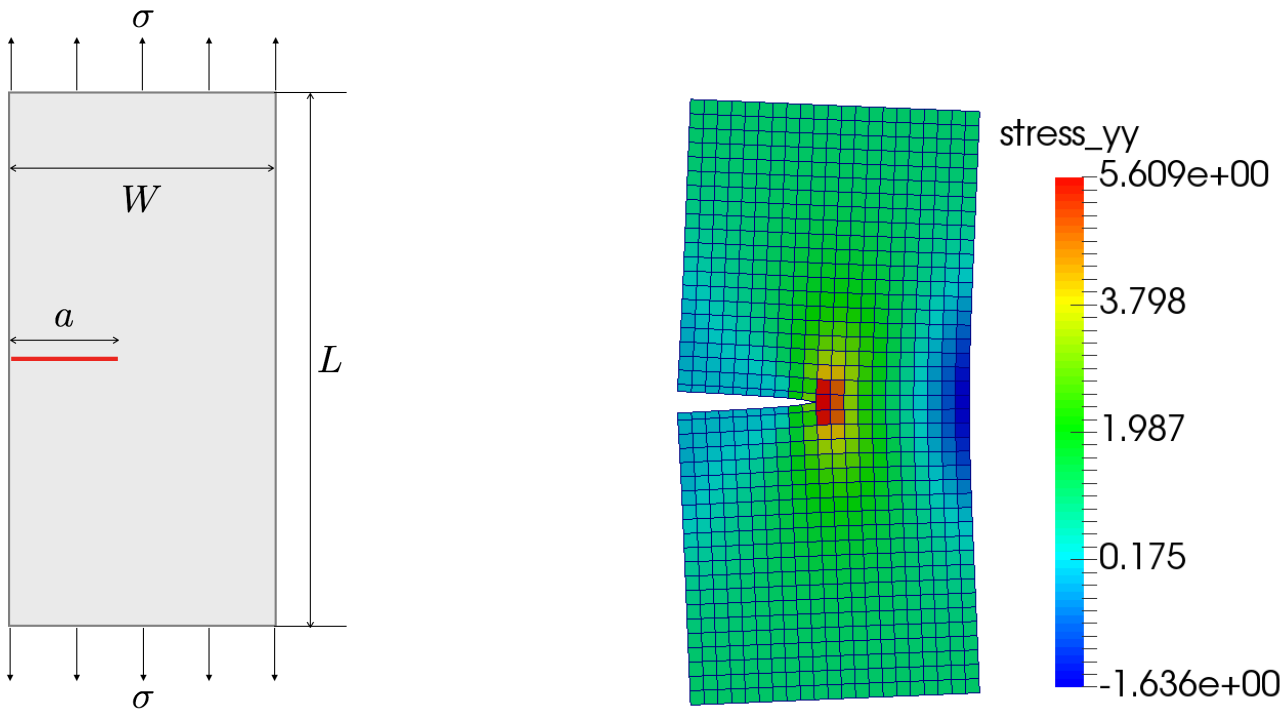

(a) (b)

Figure 10: (a) Geometry of 2D edge crack problem (b) The contour of σ_{yy}

4.3.2 3D penny crack

We next consider a circular penny crack embedded in a domain subjected to far-field tension, in which case the loading is pure Mode-I. The Young's modulus of the material is 1000,000 and Poisson's ratio is 0.3. The radius of the crack was taken to be of length $r = 0.5$. A constant normal traction of 1 is applied to the top surface.

We compare results to the analytical solution to this problem for a penny-shaped crack in an infinite domain. The analytical solution is given as $K_I = 2.213\sigma\sqrt{r/\pi}$. The results are shown in Figure 12 with mesh size $51 \times 51 \times 51$. We notice that on this relatively coarse mesh, the X-FEM approximation with near-tip enrichment gives very good accurate K_I. Furthermore, the oscillation behavior is no longer observed by using the near-tip enrichment due to the better representation of the crack front geometry.

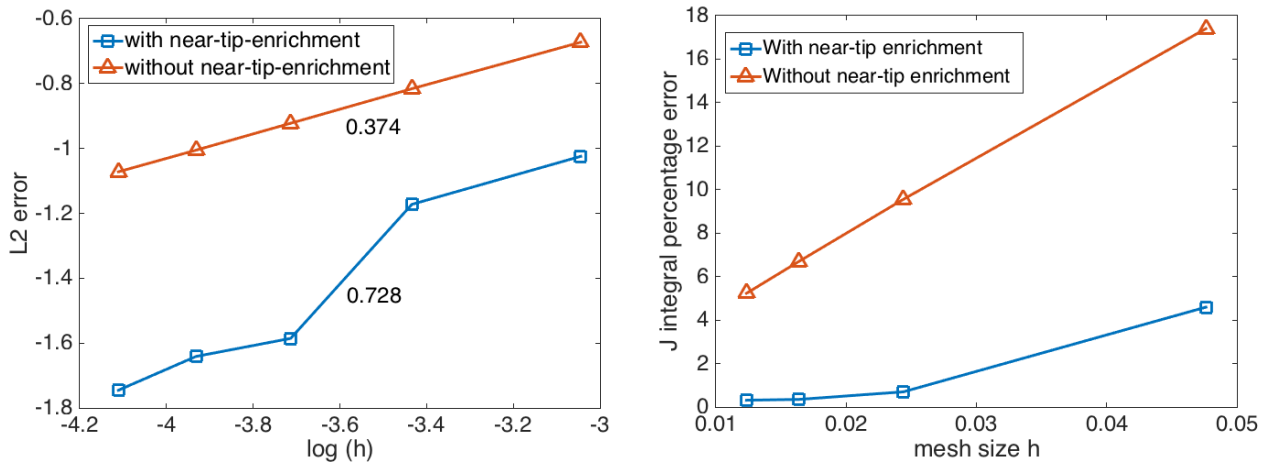

(a) (b)

Figure 11: (a) Convergence study of σ_{yy} (b) Convergence study of J-integral

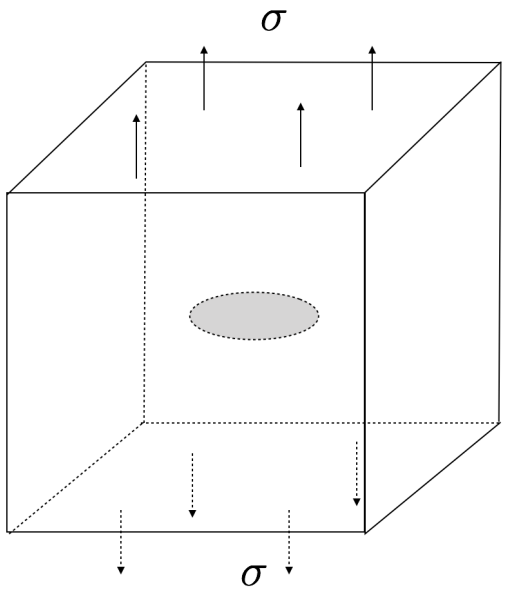

Figure 12: Penny crack example.

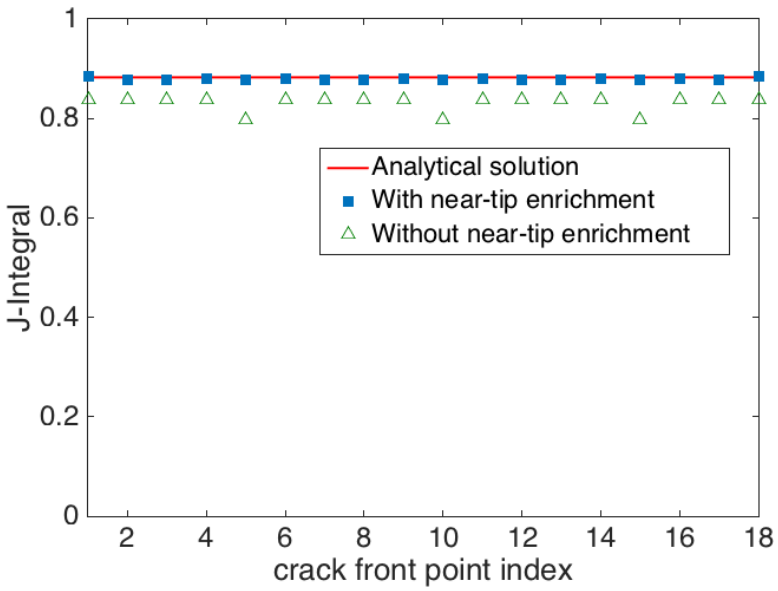

Figure 13: Variation of K_I along the crack front for a flat, penny-shaped crack subjected to pure Mode-I loading. Results were obtained using $51 \times 51 \times 51$ structured Cartesian mesh.

5 Summary

Advances have been made to the engineering-scale fracture mechanics capability for evaluation of RPV integrity under transient loading in Grizzly.

The capabilities for probabilistic fracture mechanics evaluation of a population of flaws has been included in Grizzly version 1.5. A modular, object oriented framework for the various aspects of this computation has been developed in Grizzly. This allows for a wide variety of techniques to be used to evaluate embrittlement, fluence, far-field stresses applied to a flaw, and stress intensity factors. This capability will be further refined and tested in preparation for the 2.0 release of Grizzly in Fiscal Year 2018.

A general procedure to generate coefficients for a reduced order model of a detailed flaw geometry has been developed and demonstrated. This permits the representation of arbitrary flaw geometries at arbitrary orientations. This approach is flexible, and far more efficient that direct evaluation of fracture parameters during a transient event using a finite element model.

The XFEM capability in Grizzly has been expanded to permit including the higher-order terms in solution fields near the crack tip. This has been demonstrated to give better convergence rates and significantly decreases the noise observed in the fracture solution along the crack tip in XFEM simulations.

The combination of these developments brings Grizzly closer to a state where it can be applied in production as a general tool for engineering-scale fracture mechanics analysis. The 1.5 version of Grizzly is a testing release, but a version including capabilities prepared for production use is planned for the 2018 fiscal year.

As new and refined models for predicting the progression of embrittlement are developed, these will be implemented and made available in Grizzly for use within this engineering-scale fracture mechanics framework. Grizzly is the tool that will facilitate the delivery of advances in understanding of RPV material microstructure and engineering property evolution made by the LWRS program to end users.

6 References

[1] B. W. Spencer, M. Backman, P. T. Williams, W. M. Hoffman, A. Alfonsi, T. L. Dickson, B. R. Bass, and H. B. Klasky. *Probabilistic Fracture Mechanics of Reactor Pressure Vessels with Populations of Flaws*. Tech. rep. INL/EXT-16-40050. Idaho Falls, ID: Idaho National Laboratory, Sept. 2016.

[2] P. Williams, T. Dickson, B. R. Bass, and H. B. Klasky. *Fracture Analysis of Vessels – Oak Ridge, FAVOR, v16.1, Computer Code: Theory and Implementation of Algorithms, Methods, and Correlations*. Tech. rep. ORNL/LTR-2016/309. Oak Ridge, TN: Oak Ridge National Laboratory, Sept. 2016.

[3] E. Eason, G. Odette, R. Nanstad, and T. Yamamoto. "A physically-based correlation of irradiation-induced transition temperature shifts for RPV steels". In: *Journal of Nuclear Materials* 433.1-3 (Feb. 2013), pp. 240–254.

[4] H. F. Bückner. "A novel principle for the computation of stress intensity factors". In: *Z. angew Math. Mech.* 50 (1970), pp. 529–546.

A Benchmarking of Reduced Order Fracture Models for Axis-Aligned Flaws

The Grizzly reduced order models for axis aligned flaws are based on those in the FAVOR code. FAVOR uses a library of previously determined influence coefficients in order to obtain solutions. This library of existing solutions has already been verified by the FAVOR development team, so FAVOR results are useful for benchmarking the Grizzly implementation of the axis-aligned reduced order models.

A set of 81 unique flaws were evaluated using both FAVOR and Grizzly. Those specific flaws were chosen because their solutions did not require interpolation. Nearly every flaw evaluated in this benchmarking effort now shows near identical results between the two codes. A number of issues were identified and resolved as a result of this exercise, which was done in collaboration between the Grizzly and FAVOR development teams. One flaw geometry considered here does not show near perfect agreement between the two models. The difference in results for this instance was identified through collaboration between the two development teams. For infinite aspect ratio, circumferential, surface breaking flaws, with a relative depth of 30% or higher, FAVOR switches from the model used for shallow flaws to a legacy set of SIFICs because the FAVOR development team did not have a chance to fully test the SIFIC model under those conditions. This does not represent an implementation error in Grizzly, but simply a different modeling choice.

A small subset of the flaws used in the benchmarking effort are shown in the following figures. This sample of plots is representative of the wide range of flaw geometries considered as well as the close agreement between the two codes.

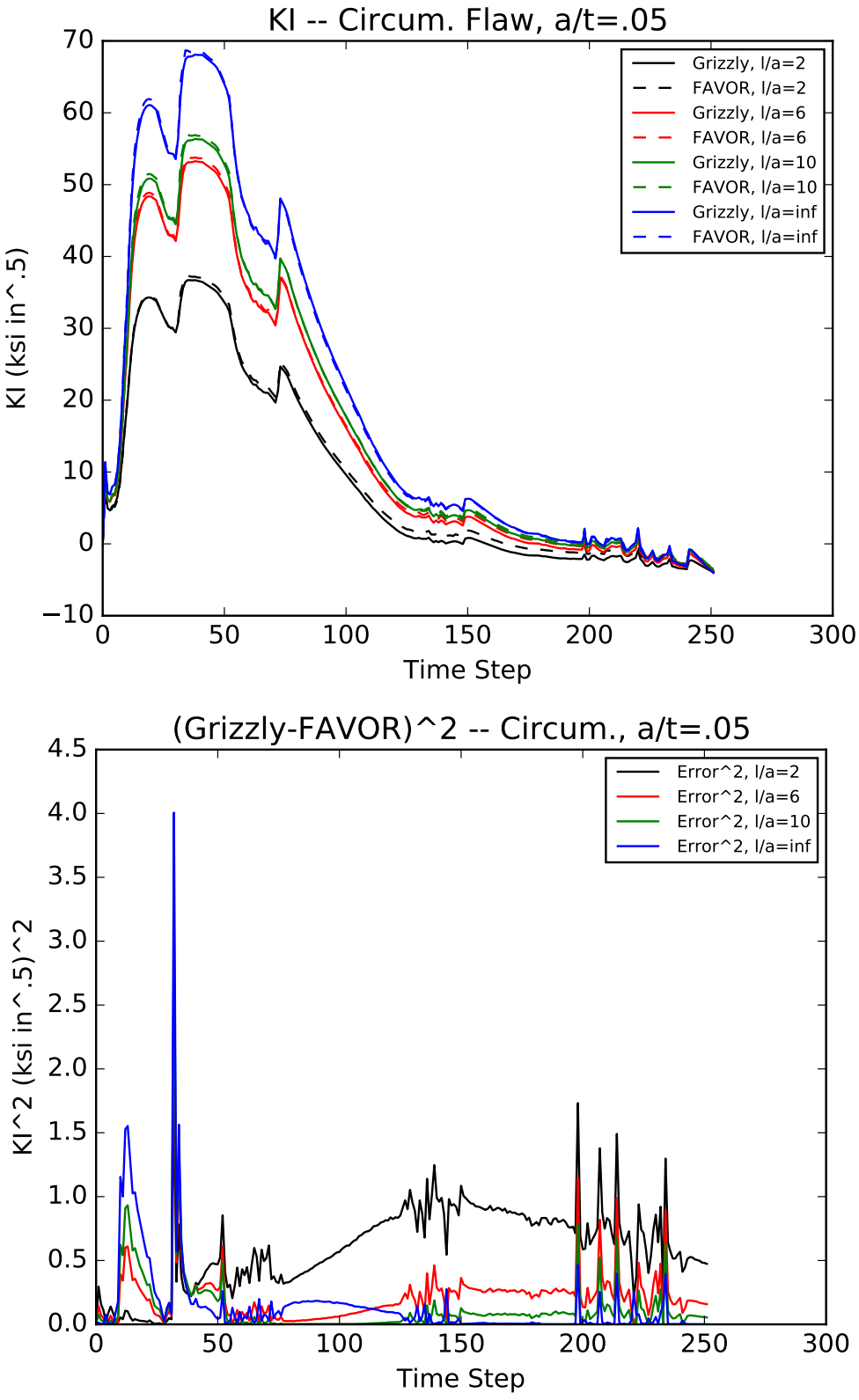

Figure 14: Circumferential, Surface Breaking Flaw, Relative depth = 5%

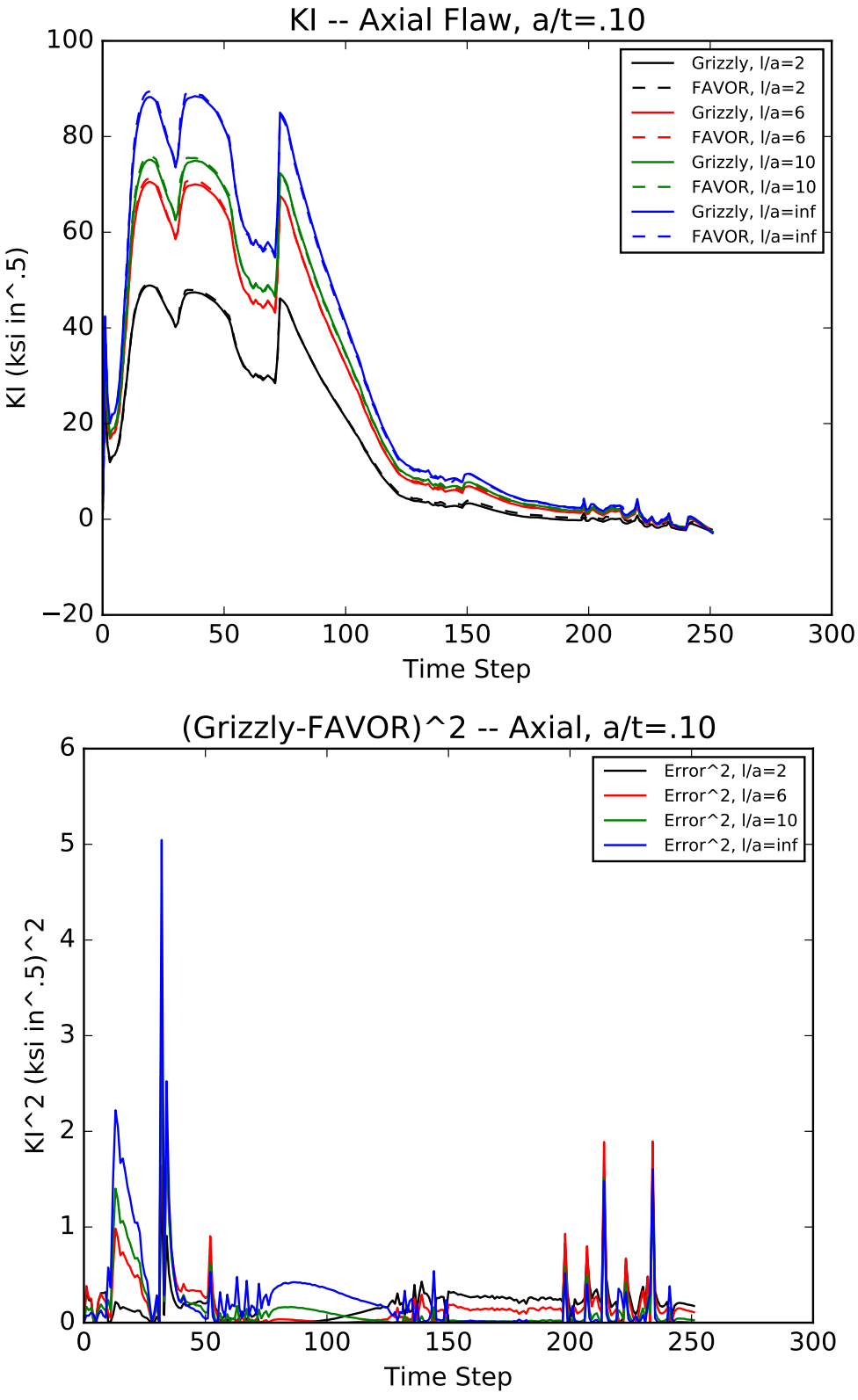

Figure 15: Axial, Surface Breaking Flaw, Relative depth = 10%

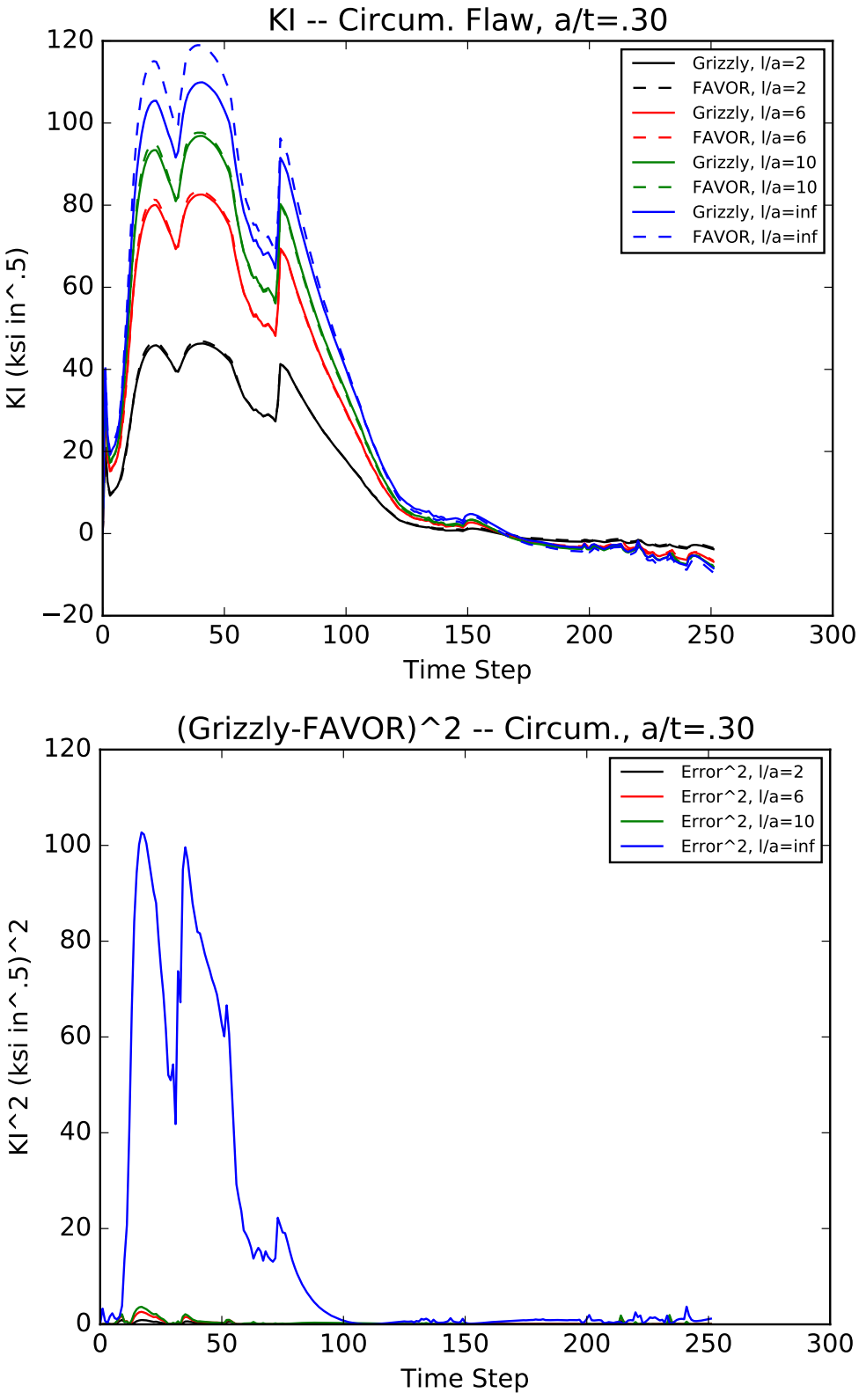

Figure 16: Circumferential, Surface Breaking Flaw, Relative depth = 30%

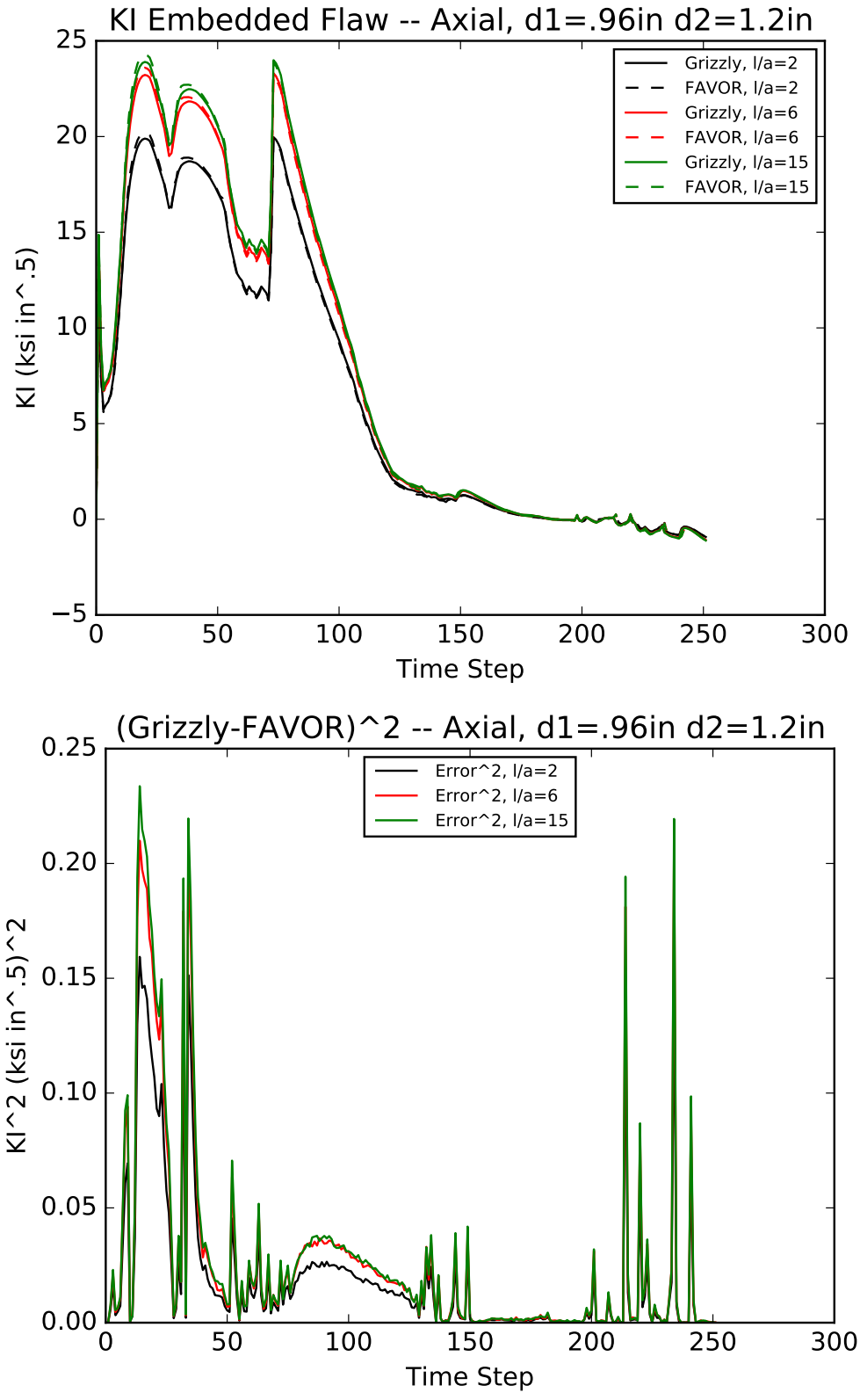

Figure 17: Axial, Embedded Flaw

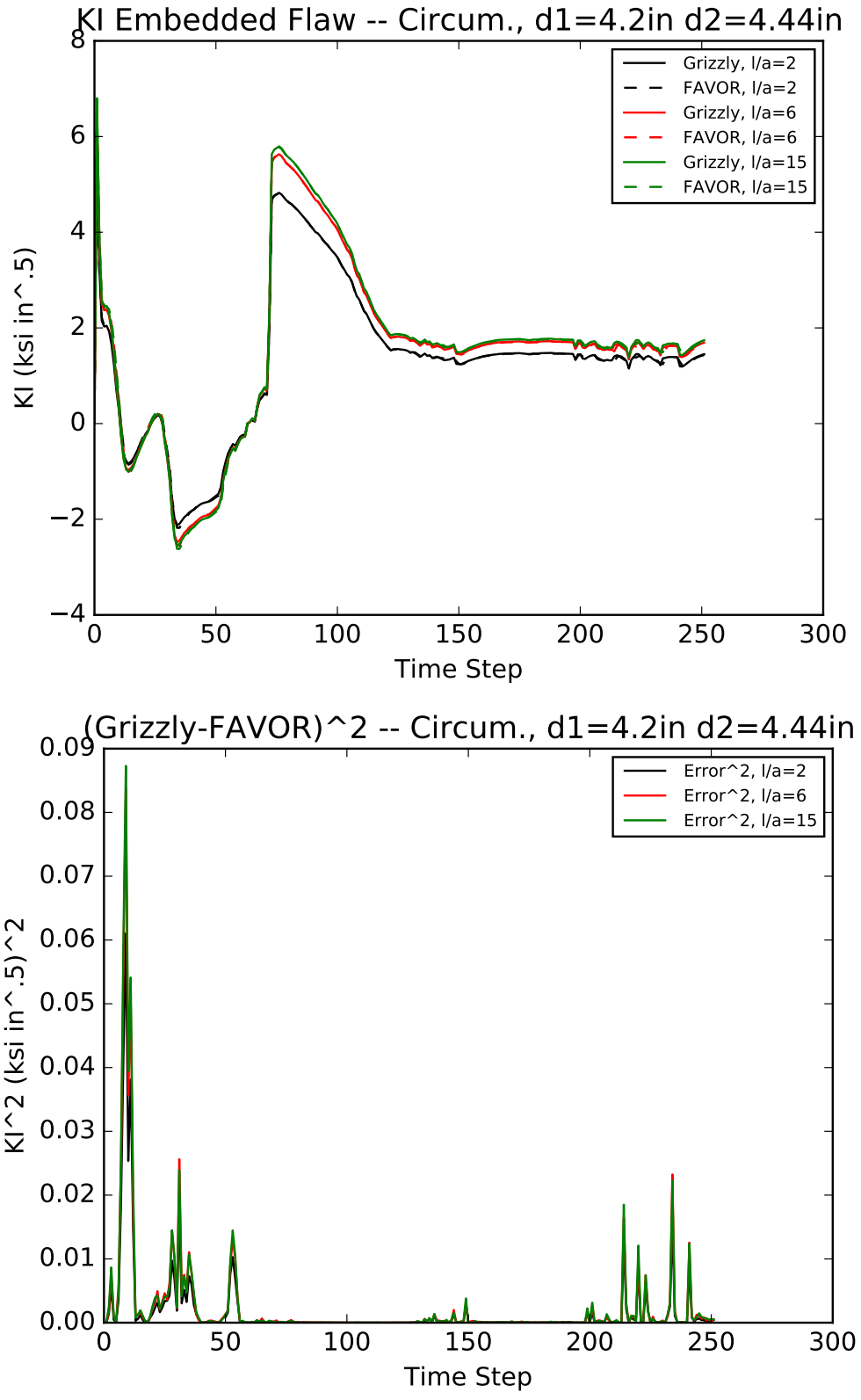

Figure 18: Circumferential, Surface Breaking Flaw

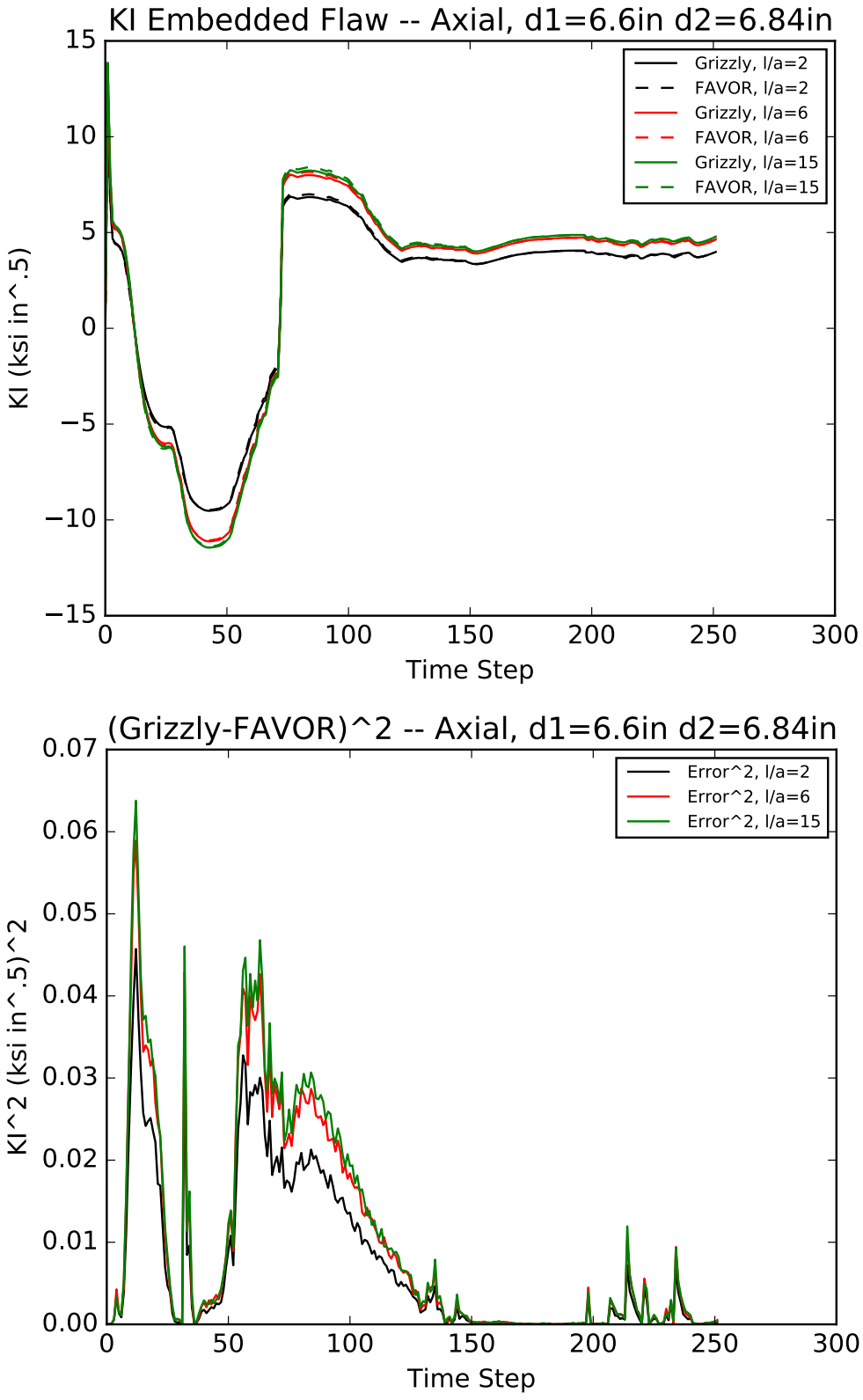

Figure 19: Axial, Surface Breaking Flaw